Glacial ripping: geomorphological evidence from Sweden for a new process of glacial erosion

Adrian M. Hall , Maarten Krabbendam , Mikis van Boeckel , Bradley W. Goodfellow , Clas Hättestrand , Jakob Heyman , Romesh N. Palamakumbura , Arjen P. Stroeven & Jens-Ove Näslund

Published online: 05 Jun 2020.

Submit your article to this journal ☑

Article views: 1426

View related articles ☑

View Crossmark data ☑

Citing articles: 1 View citing articles ☑

Glacial ripping: geomorphological evidence from Sweden for a new process of glacial erosion

Adrian M. Hall[a], Maarten Krabbendam[b], Mikis van Boeckel[a], Bradley W. Goodfellow[c], Clas Hättestrand[a], Jakob Heyman[d], Romesh N. Palamakumbura[b], Arjen P. Stroeven[a,e] and Jens-Ove Näslund[f]

[a]Geomorphology & Glaciology, Department of Physical Geography, Stockholm University, Stockholm, Sweden; [b]British Geological Survey, The Lyell Centre, Research Avenue South, Edinburgh, UK; [c]Geological Survey of Sweden (SGU), Lund, Sweden; [d]Department of Earth Sciences, University of Gothenburg, Gothenburg, Sweden; [e]Bolin Centre for Climate Research, Stockholm University, Stockholm, Sweden; [f]Svensk Kärnbränslehantering AB (SKB), Solna, Sweden

ABSTRACT

In low relief Precambrian gneiss terrain in eastern Sweden, abraded bedrock surfaces were ripped apart by the Fennoscandian Ice Sheet. The resultant *boulder spreads* are covers of large, angular boulders, many with glacial transport distances of 1–100 m. Boulder spreads occur alongside partly disintegrated roches moutonnées and associated fracture caves, and are associated with *disrupted bedrock*, which shows extensive fracture dilation in the near surface. These features are distributed in ice-flow parallel belts up to 10 km wide and extend over distances of >500 km. Our hypothesis is that the assemblage results from (1) hydraulic jacking and bedrock disruption, (2) subglacial ripping and (3) displacement, transport and final deposition of boulders. Soft sediment fills indicate jacking and dilation of pre-existing bedrock fractures by groundwater overpressure below the ice sheet. Overpressure reduces frictional resistance along fractures. Where ice traction overcomes this resistance, the rock mass strength is exceeded, resulting in disintegration of rock surfaces and ripping apart into separate blocks. Further movement and deposition create boulder spreads and moraines. Short boulder transport distances and high angularity indicate that glacial ripping operated late in the last deglaciation. The depths of rock mobilized in boulder spreads are estimated as 1–4 m. This compares with 0.6–1.6 m depths of erosion during the last glaciation derived from cosmogenic nuclide inventories of samples from bedrock surfaces without evidence of disruption. Glacially disrupted and ripped bedrock is also made ready for removal by future ice sheets. Hence *glacial ripping* is a highly effective process of glacial erosion.

Introduction

For almost 200 years, the main processes of glacial erosion have been regarded as plucking (quarrying) and abrasion, aided by erosion by subglacial meltwater (Chamberlin 1889; Boulton 1987; Cunningham 1990; Glasser and Warren 1990; Benn and Evans 2010; Krabbendam and Glasser 2011; Iverson and Person 2012; Alley et al. 2019). However, in lowland Sweden there are extensive

CONTACT Adrian M. Hall ✉ adrian.hall@natgeo.su.se Geomorphology & Glaciology, Department of Physical Geography, Stockholm University, 106 91 Stockholm, Sweden

fields of large boulders that are neither formed by periglacial or slope processes, nor can be explained by classic abrasion or plucking (Lagerbäck et al. 2005). In addition, many disrupted and partly disintegrated roches moutonnées have been identified in east-central Sweden, and several contain 8–10 m deep inter-block cave systems ('fracture caves'/'boulder caves') in fractured gneiss (Sjöberg 1986; Mörner et al. 2000); (Figure 1). Previously, the caves have been interpreted as caused by
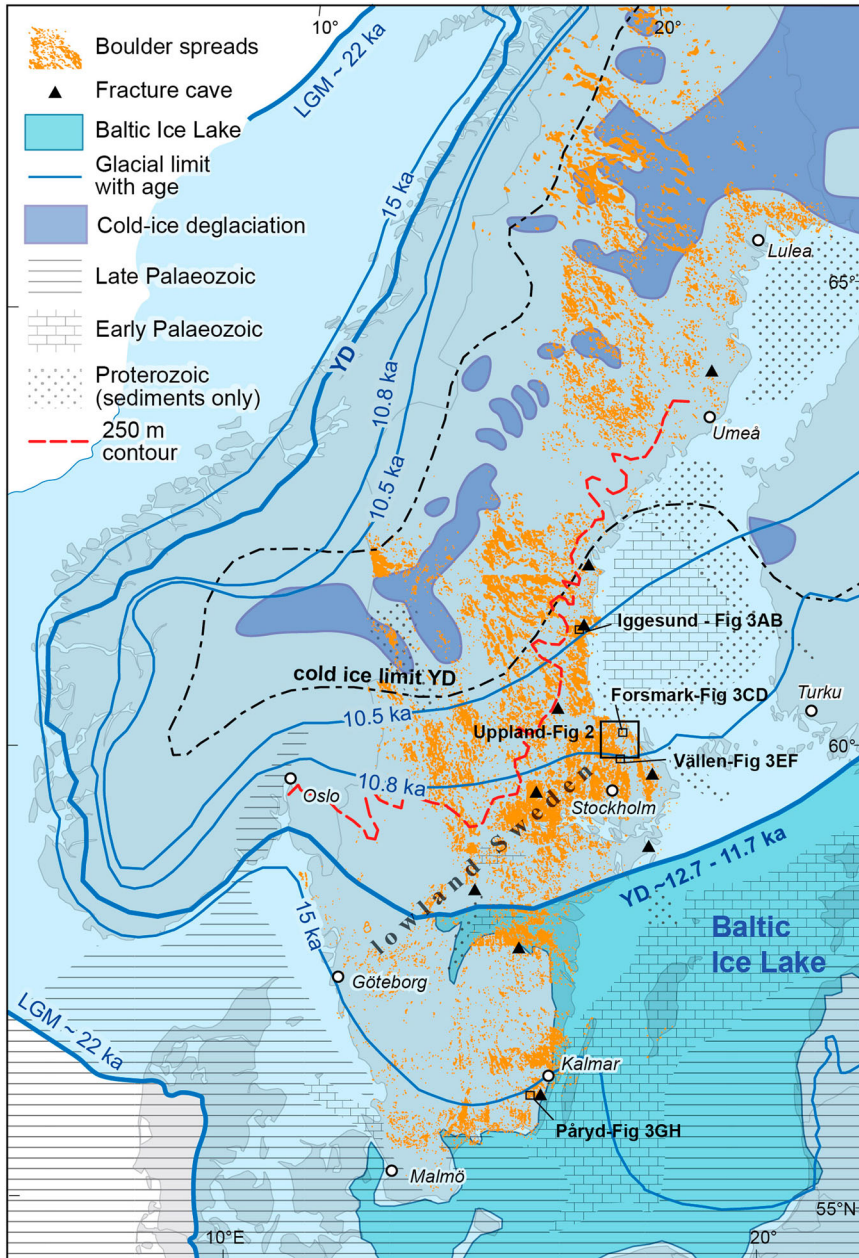
Figure 1. Overview map with selected Fennoscandian Ice Sheet margin positions, Baltic Ice Lake, minimum limit of cold-based deglaciation during the Younger Dryas (Stroeven et al. 2016), boulder spreads (SGU data), and fracture caves in partly disintegrated roches moutonnées (Sjöberg 1986). Schematic distribution of Proterozoic sedimentary rocks after Asch (2005); metamorphic and igneous rocks are not shown. YD = Younger Dryas limit. Boxes indicate the positions of Figures 2 and 4.

large magnitude (>M7) earthquakes apparently related to postglacial isostatic uplift (De Geer 1940; Mörner 1978, 2004; Mörner and Sjöberg 2018), although glacial origins have also been proposed (Lundqvist 1987; Lagerbäck et al. 2005). Also observed in central east-central Sweden are sediment-filled fractures, attributed to hydraulic jacking of bedrock fractures, and infilled with soft sediment (Carlsson 1979; Pusch et al. 1990). Lagerbäck et al. (2005) first suggested that these different phenomena were related. Here we provide critical evidence from four study areas to confirm that these phenomena are linked by a hitherto unrecognized erosion mechanism termed here *glacial ripping*. Our hypothesis is that glacial ripping is a process-sequence that involves: (1) hydraulic jacking and dilation along pre-existing fractures by over-pressured subglacial meltwater; (2) disruption and disintegration (the actual ripping) of fracture-bound blocks of bedrock by traction of the overlying ice; and (3) displacement, transport and deposition of the liberated blocks into boulder spreads. We suggest that glacial ripping operated across large parts of the hard-rock bed of the Fennoscandian Ice Sheet (FIS) in Sweden.

Setting

Eastern Sweden has been repeatedly glaciated by the FIS over the course of the Quaternary (Kleman et al. 2008). During the latest Weichselian (~Wisconsin) glaciation, the FIS reached its maximum extent in Denmark around 22 ka BP (Figure 1). Subsequently, its southern margin retreated northwards, and across eastern Sweden after 15.0 ka BP (Stroeven et al. 2016) (Figure 1). A prolonged stillstand or readvance occurred at ~12.7 ka BP, during the Younger Dryas stadial, when modelled surface ice-flow velocities were >400 m/yr (Patton et al. 2017). Its final northward retreat, after 11.7 ka BP, was rapid at 200–400 m/yr (Strömberg 1994; Stroeven et al. 2016). Retreat was by calving in a shallow lacustrine (Baltic Ice Lake) to marine-terminating setting (Lundqvist 1987, 2007; Andrén et al. 2002), with high meltwater fluxes beneath the melting ice sheet (Jansen et al. 2014; Greenwood et al. 2017). Lowland Sweden lies outside the inferred minimum extent of cold-ice bed during the Younger Dryas (Stroeven et al. 2016) (Figure 1). That the FIS in eastern Sweden remained warm-based during final deglaciation is indicated by sets of striae that link to late ice-flow directions (Kleman 1990; Stroeven et al. 2016). Late ice-flow sets formed beneath warm-based ice on the bed of the Bothnian Sea (Greenwood et al. 2017) are continuous with those in adjacent coastal area (Persson 1992; Patton et al. 2017). At the sites that we investigate here below the marine limit in eastern Sweden, available evidence strongly supports warm-based ice-flow conditions during deglaciation, consistent with the high meltwater fluxes.

The lowlands of eastern Sweden are underlain by Proterozoic gneisses of the Fennoscandian shield. The gneisses are very hard but broken along multiple sets of unevenly spaced fractures (Stephens 2010). These fractures commonly display mineral-coated surfaces resulting from several episodes of fracturing and mineralization since the onset of brittle deformation in the Mesoproterozoic (e.g. Sandström and Tullborg 2009). Hence the majority of fractures were formed prior to the Pleistocene. The gneiss basement was eroded beneath the FIS during the Pleistocene to produce rock landscapes typified by assemblages of whalebacks and roches moutonnées, separated by shallow basins and joint-guided valleys (Hall et al. 2019), similar to other glaciated shield terrains (Olvmo and Johansson 2002; Krabbendam and Bradwell 2014).

In hilly and mountainous terrain in north and west Sweden, 'surficial boulders', as mapped by the Swedish Geological Survey (SGU), may also include accumulations derived from subglacial plucking from cliffs, on boulder-rich moraines, from rockfall, or comprise periglacial block and boulder fields on mountain plateaux (Kleman and Borgström 1990). In the lowland gneiss terrain investigated here, however, cliffs are low and short and do not provide plausible sources for generating large volumes of boulders (either by plucking or rockfall). The extensive preservation of smooth, abraded rock surfaces in lowland Sweden indicates that postglacial periglacial activity did not produce periglacial blockfields at low elevations. Hence, boulder spreads in lowland Sweden cannot be

satisfactorily explained by these processes, and we focus here on these enigmatic boulder spreads found in lowland terrain.

In Uppland, and in eastern lowland Sweden generally, three different types of erosional terrain are recognized at the regional and local scales (Hall et al. 2019) (Figure 2):

(1) *Ice-roughened terrain.* In this terrain, exposed bedrock is extensive on topographic high points. Roches moutonnées and box hills with rectilinear plan forms rise to more than 10 m above their surroundings; exposed bedrock is widely abraded and few boulders occur. Fracture-guided valleys of varying widths and orientations are common. Till occurs mainly in depressions, and partly infills shallow rock basins with star- and box-shaped outlines.
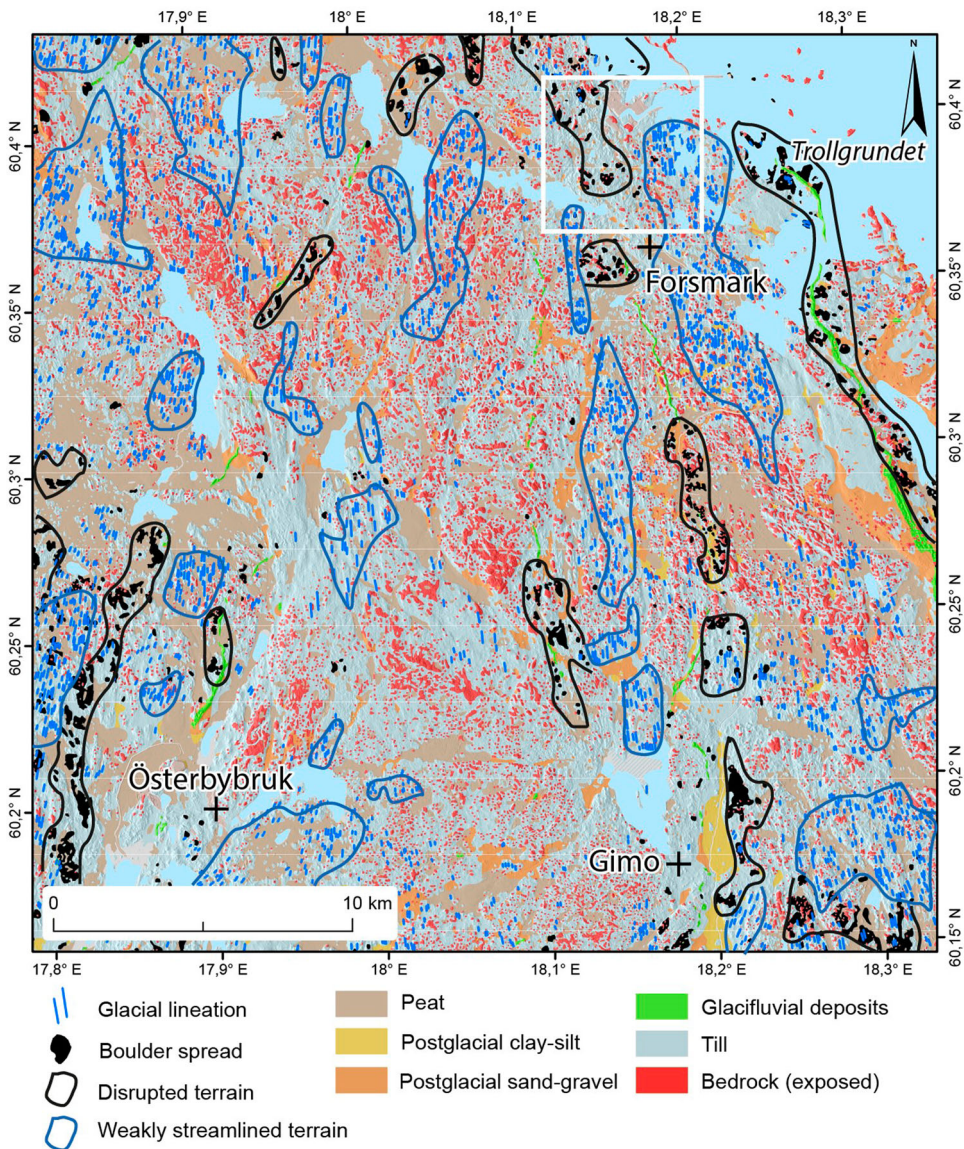
Figure 2. Quaternary geology (SGU data) and glacial bedforms in NE Uppland, including weakly streamlined and disrupted (ripped) terrain types. Roughened terrain is represented by the large areas with exposed bedrock. Area of Figure 4(C–D) indicated by white box.

(2) *Weakly streamlined terrain*. Mapping of topographic lineaments from LiDAR digital terrain models in NE Uppland indicates that patches and belts of weakly streamlined terrain exist oriented roughly parallel to ice flow. (Figure 2). In such terrain, exposed bedrock is more restricted in its extent, and till cover is more extensive. Low ridges have rock cores that show rounded stoss faces, with fracture-guided flanks and small lee side cliffs, indicating a component of plucking. Till tails of 50–300 m length, aligned parallel with former ice flow, give drumlinoid forms, giving the terrain an overall streamlined character. Broad trenches, depressions and rock basins occur in fracture zones between hill groups.

(3) *Glacially disrupted terrain*. *In situ* bedrock with glacially abraded surfaces is not widely exposed and boulder spreads are extensive (Figures 2 and 3). Remaining roches moutonnées often show disruption, loss of blocks from sockets, and lee- and flank-side boulder trains. It is this terrain that we examine in this paper.

Methods, datasets and terminology

Maps from SGU show 'surficial boulders' covering large areas of Sweden (Figure 1). Boulder spreads are commonly concealed by forest, so our work focussed on recently clear-felled areas. Boulder spreads are poorly imaged in digital terrain models but are visible in clear-felled areas on orthorectified aerial photographs from Lantmäteriet – the Swedish mapping, cadastral and land registration authority (Figure 3). Our field mapping focussed on four areas in eastern Sweden where boulder spreads are extensive: Iggesund in Gävleborg county, Forsmark and Lake Vällen in Uppland county, and Påryd in Kalmar county (Figure 1). In each study area, we recorded and mapped characteristics of boulder spreads: depth and lateral extent; clast size, shape, and lithology; transport distance from source rock units; and relationships with glacial landforms, such as moraines and eskers. Near Forsmark, we report a ground survey of a boulder spread at Gunnarsbo, in part using low-altitude orthorectified aerial photographs taken by an unmanned aerial vehicle.

We use the term '*boulder spread*' to distinguish them from *blockfield*s, which are generally seen to develop by periglacial freeze–thaw action (e.g. Rea et al. 1996; Goodfellow et al. 2009). We use the term 'block' if the fracture-bounded rock block is still *in-situ*, or almost so. Once a block has been separated from its neighbours and removed from its socket, it becomes a 'clast'. In terms of clast size, we use 'boulder' for clasts with b-axis lengths between 0.256 and 4.1 m; clasts with a b-axis larger than 4.1 m are termed 'mega-clasts' (Terry and Goff 2014). Due to postglacial emergence, there is a potential bias in observed boulder size distributions caused by selective reworking by marine wave erosion. On the present Baltic shoreline, we observe that boulders >0.8 m in b-axis length have not been moved by wave action but smaller boulders are locally transported by storm waves to form clusters, spreads and ridges. We assume that boulders >0.8 m were not reworked during post-glacial emergence.

To understand the process of bedrock disruption, we provide a structural analysis of the large (~5000 m^2) disintegrated roche moutonnée at Bodagrottorna near Iggesund (Figure 1). The results are compared with other examples of disrupted and disintegrated bedrock hills that occur in association with boulder spreads in the study areas in Uppland and Kalmar counties (Figure 1).

Boulder spreads and disintegrated bedrock hills are commonly found in association with *jacked* and *disrupted bedrock*, where the rock mass has been disturbed, with dilation of rock fractures and slight displacement of blocks. Jacking and disruption were documented during excavations in the 1970s at the Forsmark nuclear power plant site (Carlsson 1979; Carlsson and Christiansson 2007). As part of our surveys of large quarries in each study area, we report on results from the Runtorp Quarry, Påryd (Figure 1).

We combine our new field evidence for boulder spreads, disintegration of roches moutonnées and rock disruption with existing information on boulder spreads from SGU maps and on jacked and
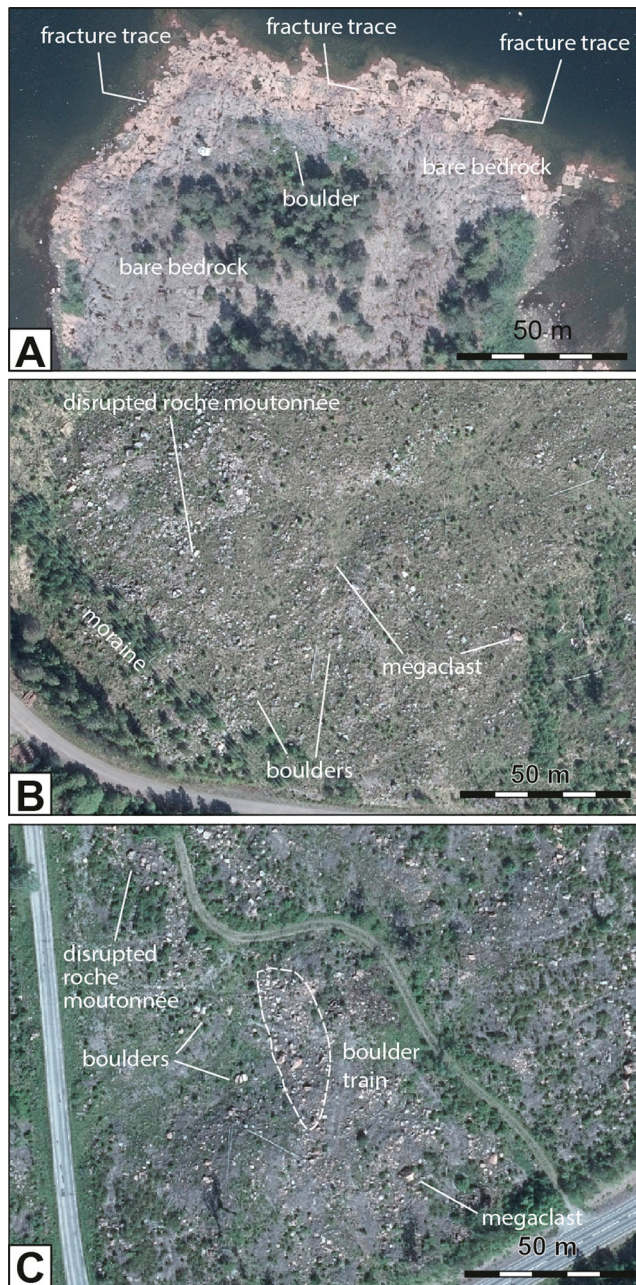
Figure 3. Contrasting rock surfaces without and with boulder spreads, showing the different density of boulders at the surface. Aerial photos from Lantmäteriet. (A). Abraded and plucked bedrock surface within weakly streamlined terrain and lacking in boulder spreads at Stånggrundet, c. 3 km east the Forsmark power station (Lat. 60.398645°N; Long. 18.222194°E). (B) Gunnarsbo boulder spread, c. 300 m west of the Forsmark power station (Lat. 60.402475°N; Long. 18.144887°E). (C) Boulder spread c 1 km SSE of Bladåker, near Lake Vällen (Lat. 59.991028° N; Long. 18.269045°E).

disrupted bedrock and boulder spreads in Swedish Nuclear Fuel and Waste Management Company (SKB) reports from the Forsmark area. This compilation presents evidence at the regional (1–10 km), local (0.1-1 km) and macro- (10-100 m) scales and allows us to present the hypothesis that glacial ripping involves a process sequence of jacking, disruption and disintegration,

entrainment, transport and deposition. Recent reporting of cosmogenic nuclide results from undisrupted rock surfaces around Forsmark (Hall et al. 2019) allows preliminary comparisons of the depths of rock removed by abrasion and plucking during the last glaciation with those lost to ripping.

Results

Boulder spreads

Our field observations in lowland eastern Sweden are consistent with SGU mapping and early reports (Lundqvist 1940; Lundqvist 1986) of 'surficial boulders' and 'large surficial boulders' (on Swedish maps: blockig yta; storblockig yta). Hence, we equate these mapped distributions with *boulder spreads* as described herein. Individual boulder spreads comprise many (n>100) angular boulders and occasional mega-clasts which form rough ground that is largely used for forestry.

In Uppland, boulder spreads occur in 2-10 km wide patches and belts that lie broadly parallel to former N-S ice flow (Figures 1 and 2). Boundaries to individual boulder spreads are generally sharp (Figures 2 and 3). Boulder spreads are rare or absent in zones of roughened and weakly streamlined bedrock terrain (Figure 2). Belts with boulder spreads are developed in different gneiss lithologies and across variably spaced vertical fractures in low (<20 m) relief rock terrain (Hall et al. 2019), indicating a lack of geological and topographical control at regional scales.

Boulder spreads extend for >500 km along the length of Sweden but are discontinuous (Figure 1). The largest areas of boulder spreads lie within the Younger Dryas limits of the FIS (Figure 1). Boulder spreads may be of regional extent, covering areas of >50 km^2 around Iggesund (Figure 4(A, B)) and Lake Vällen (Figure 4(E, F)). Around Forsmark, the boulder spreads occur as patches <0.5 km^2 in an area associated with partly disrupted bedrock hills that are 3-10 m high (Figure 4(C, D)). At Runtorp, boulder spreads also occur in patches but within terrain with extensive, thin till cover (Figure 4 (G, H)). Within boulder spreads, bedrock outcrops are typically small in area and widely spaced (Figure 3).

Boulder spreads are observed to rest on disrupted bedrock, on till or, less widely, on bare, intact rock surfaces. On lee-sides and oblique scarps, thicker stacks of boulders occur (3–5 boulders deep). At two sites, Njutånger, Iggesund (Figure 1) and Trollgrundet, Forsmark (Figure 2), boulder spreads are overlain by eskers and so predate esker formation. Angular, locally sourced boulders form low (1–5 m high) moraine ridges and hummocks indicating a form of reworking; specific examples are found near Iggesund (Figure 5(F)).

One typical boulder spread was analysed in detail at Gunnarsbo (Figure 6). The boulder spread comprises a 1-3 m thick, boulder-rich rubble layer. Most boulders are angular to very angular, with b-axes of 1–3 m and approximately cuboid. Transported groups of angular boulders retain clearly identifiable fractured surfaces, marked with fracture coatings, and glacially abraded surfaces, commonly with clearly recognizable glacial striae. Orientations of amphibolite foliation and glacial striae were measured on boulders and compared with adjacent bedrock outcrops, indicating substantial boulder rotations (>45°; Figure 6(D, E)). Boulder size and shape mimic fracture-bound block patterns in the adjacent bedrock outcrops. Approximately 90% of the boulders are of amphibolite. Some 10% or less of the boulders are of different lithologies (various types of granitic/felsic gneisses) and are erratic: these boulders are typically more rounded. Small areas of disrupted but essentially intact amphibolite outcrops were identified by the presence of upper striated surfaces and by gneissic foliation with the same orientations as adjacent *in situ* bedrock. The boulder spread overlies a mapped body of amphibolite, with a width (along ice flow) of ~3 km; (Figure 6(A)), so that *maximum* boulder transport distance is 3 km. Within the Gunnarsbo boulder spread, some individual boulders with distinctive lithologies and textures can be traced to bedrock sources, indicating transport distances <10 m. Hence, many boulders in this spread have been transported over short distances.

The main characteristics of the Gunnarsbo boulder spread are widely replicated at other sites. Where boulder spreads occur on gneisses of varied lithology, as around Lake Vällen (Lagerbäck
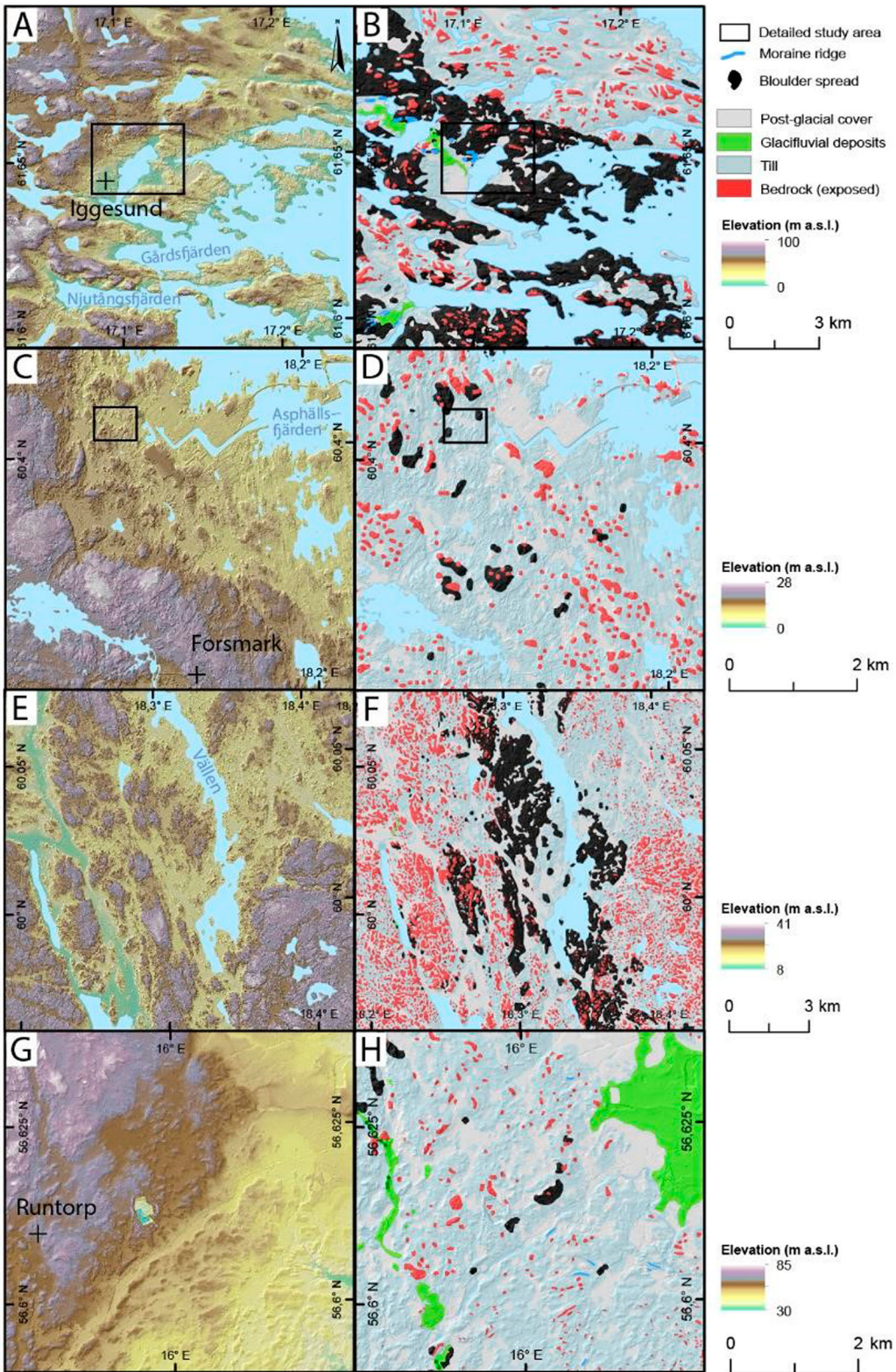
Figure 4. Relief (Lantmäteriet data) and Quaternary geology (SGU data) of four study areas: A-B. Iggesund. C-D. Forsmark. E-F. Lake Vällen. G–H. Påryd area, with Runtorp Quarry. See Figure 1 for the locations of these areas. Boxes in panels A–B and C–D, refer indicate locations of detailed study areas shown in Figures 5 and 6, respectively.
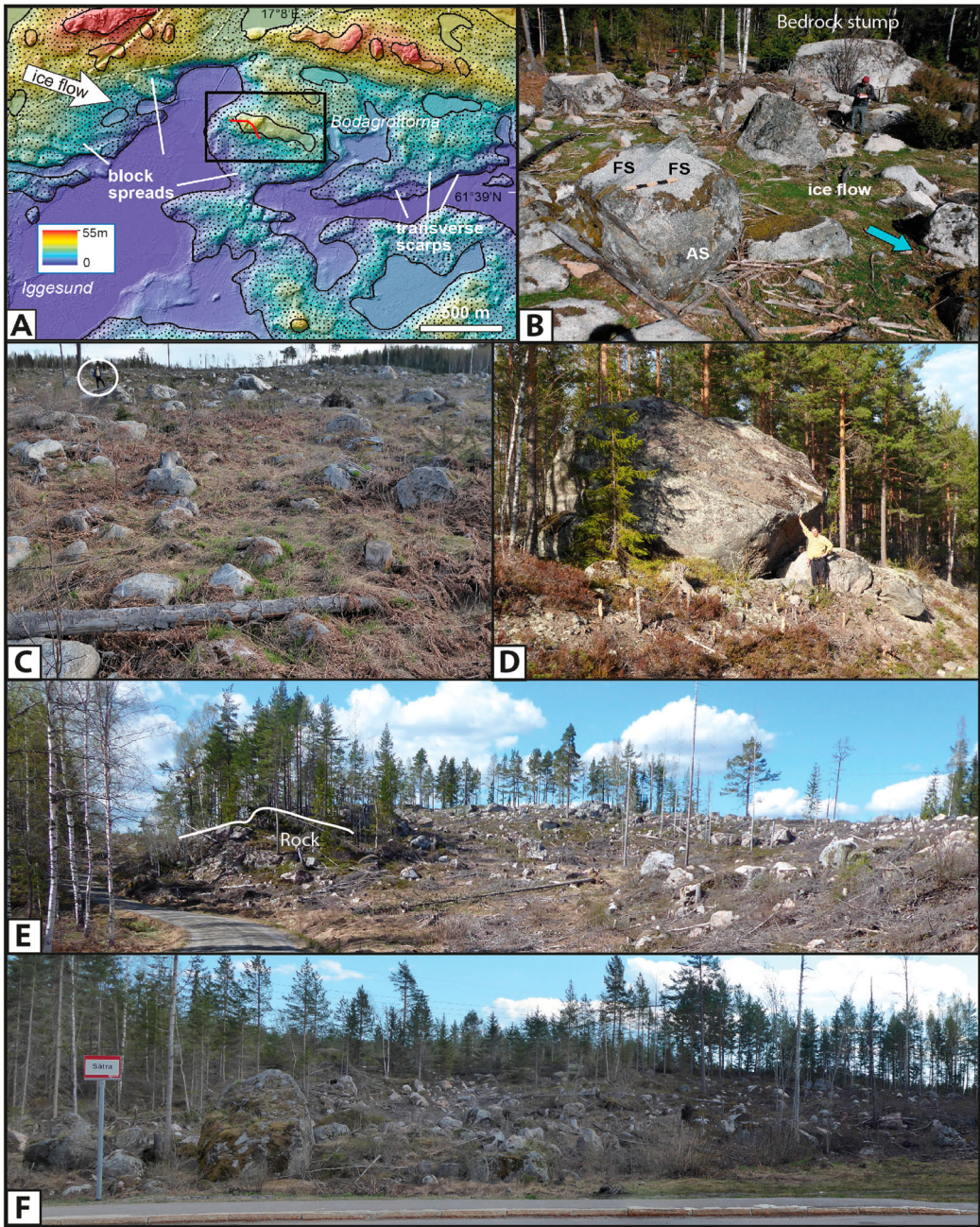
Figure 5. Boulder spreads at Iggesund. A. DEM of an area NE of Iggesund, including the study area around Bodagrottorna cave (cf. Figure 7, red line denotes the location of transect shown in Figure 7(B)). B. Outcrop and part of its boulder spread on the western flank of the hill (Lat. 61.653454°N; Long. 17.124782°E). AS = abraded surface; FS is fracture surface / joint. C. Boulder spread in a clear-cut area of former forest north of Iggesund (Lat. 61.657269°N; Long. 17.088593°E); see circled person for scale. D. Mega-clast north of Bodagrottorna (Lat. 61.657360°N; Long. 17.126982°E). E. Boulder spreads resting on a bedrock ridge near Sätra, Enånger (Lat. 61-558600°N; Long. 17.015731°E). F. Moraine ridge within boulder spread at same locality.

et al. 2005) (Figures 3(C) and 4(F)), boulder lithology varies with the subjacent bedrock and indicates very local (<100 m) sourcing. At multiple sites around Forsmark, spreads and trains of angular boulders are found surrounding intact rock outcrops (Figures 3(B) and 4 (D)) and here also boulder
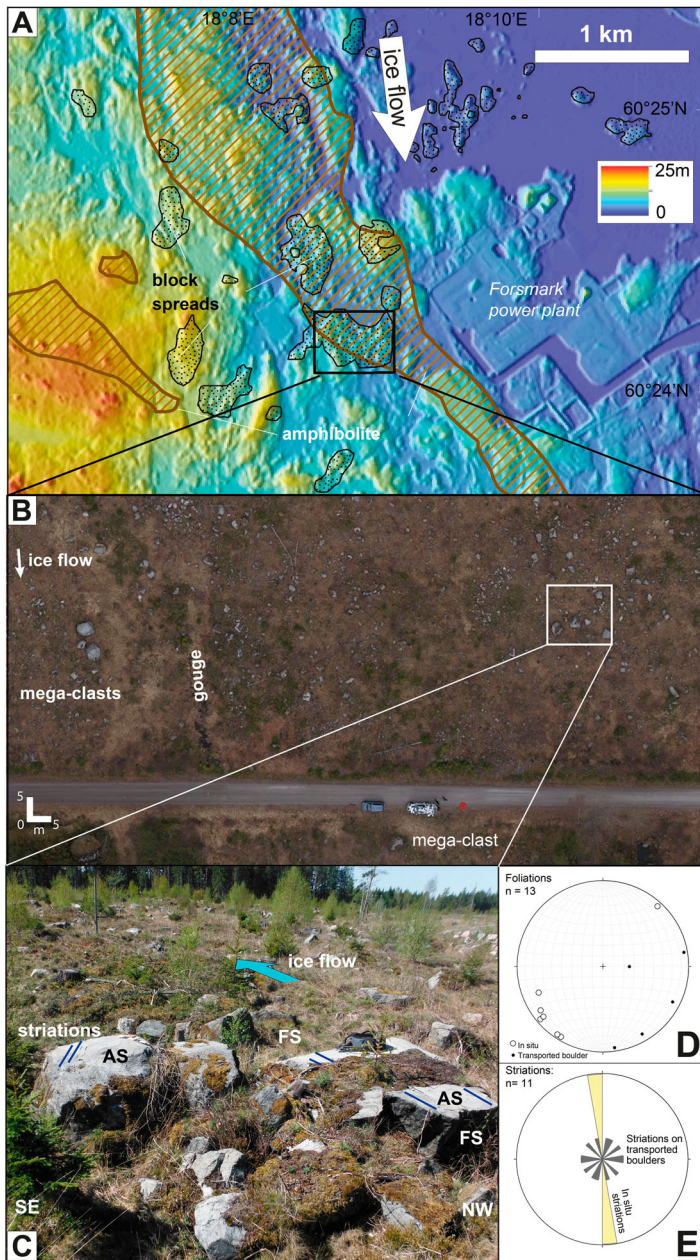
Figure 6. Boulder spreads at Forsmark. A. Boulder spreads in the area around Forsmark. Mapped amphibolite in brown hatching. Box indicates detailed study area at Gunnarsbo. B. Drone image of boulder spreads at Gunnarsbo. Box shows location of the image below. C. Individual boulders, with measured striae and abraded surfaces. AS = abraded surface; FS = fracture surface. D. Stereogram with poles of foliation surfaces for different boulders at Gunnarsbo. E. Rose diagram of measured glacial striae on boulders, with regional ice flow from striae on bedrock outcrops.

rock type is generally identical to that of adjacent bedrock found within 25 m. On the flank of the hill at Bodagrottorna, disrupted bedrock occurs within a boulder spread that forms a short (150 m) boulder train (Figure 5(B)). Our observations show that the density, high angularity and uniform, locally sourced lithologies of the boulder spreads contrast strongly with the greater roundness and
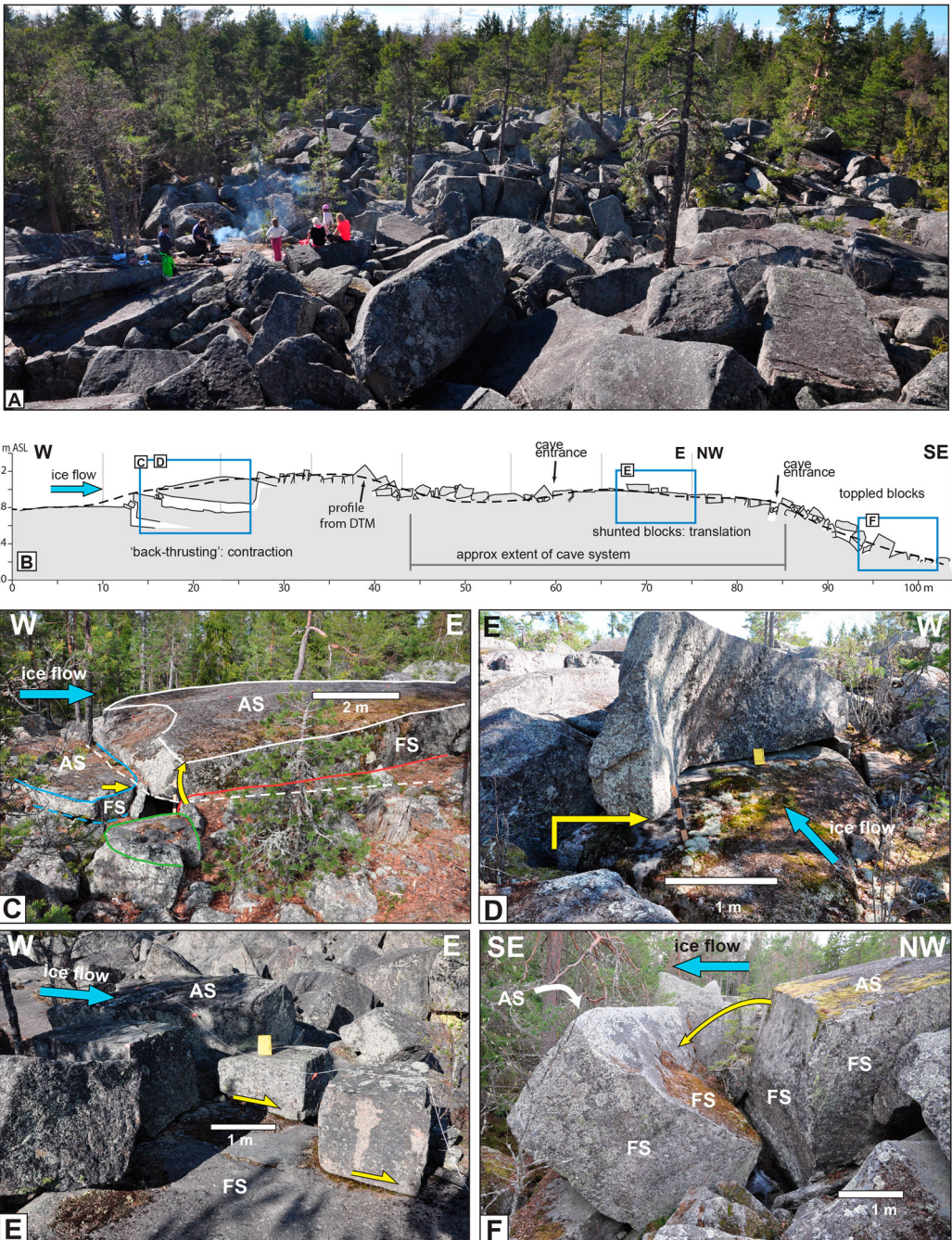
Figure 7. Disrupted roche moutonnée at Bodagrottorna, Iggesund. A. View across the disrupted and ripped surface of the roche moutonnée. B. Cross-section of the disrupted roche moutonnée. Section line shown in red on Figure 5(A. C, D). Rock slabs uplifted and 'back thrusted' against ice flow. E: Blocks shunted along subhorizontal fracture surface. F: Blocks toppled; note that the view is inverted with respect to cross-section. Yellow arrows: inferred relative block movements; coloured lines in (C) are outlines of blocks, with dashed lines below ground surface. AS = glacially abraded surface; FS = fracture surface.

more varied lithology of sparse erratic boulders and till clasts. Erratic surface boulders and till boulder clasts at Forsmark have substantially longer transport distances (typically 0.5–8 km) from source outcrops (Bergman and Hedenström 2006).

Disintegrated roches moutonnées

A number of disintegrated roches moutonnées, associated with 'fracture caves', have been noted previously (Sjöberg 1986; Mörner et al. 2000). Here, we focus on the extensive (~5000 m^2) Bodagrottorna (or Boda) roche moutonnée developed in gneissic granodiorite (Wänstedt 2000). The locality lies within a ~10 km^2 area of boulder spreads in which undisrupted bedrock outcrops cover <1% of the ground (Figure 5(A)). At Boda, the sizes of the fracture-bound blocks range from 1 to 7 m (Figure 7). Glacially abraded and fracture surfaces can be readily identified, and aid in partial restoration of block movement. Our analysis comprises a detailed cross-section of this hill (Figure 7(A, B)) and shows:

(1) On the W stoss side, blocks are shunted by back-thrusting along gently inclined fractures, suggesting a contractional ('push') regime (Figure 7(C and D));
(2) On the flatter top of the hill, a zone of horizontally translated blocks occurs, akin to normal 'plucking', without much tilting, indicating a regime of traction. Here several blocks have been removed and the top of the hill comprises fracture surfaces rather than glacially abraded tops (Figure 7(E));
(3) On the SE or lee side, numerous blocks show substantial tilting and toppling, indicating an extensional ('pull') regime (Figure 7(F)).

Fracture-bound blocks have moved along sub-horizontal fractures (SHFs) at several depths, creating voids to a maximum depth of 9 m (Carlsten and Stråhle 2000), linked together to form the cave system (previously documented by Mörner et al. 2000). The asymmetry of the three zones is consistent with ice-flow direction, indicating that traction by moving ice is the key mechanism for block displacement.

A train of mega-clasts sourced from the lee side of the hill at Bodagrottorna extends S to SE for 300 m, consistent with local ice-flow direction (Lagerbäck et al. 2005). Boulder trains 40–250 m long are also recorded down-ice from other disrupted roches moutonnées in each study area.

Around Påryd, SGU mapping indicates extensive till cover (Figure 4(H)), but sections in road cuts and at Runtorp quarry (Figure 8(E)) show many partly disrupted small (<5 m high) roches moutonnées from which large blocks have been removed and deposited as boulders and mega-clasts on till at short distances from sources. Here and around Forsmark, small roches moutonnées and whalebacks show transitions from minor disruption, with pull-apart along vertical fractures and removal of blocks from stoss-, flank- and lee-side locations, through to general disintegration. Block loss from roches moutonnées generates ribbed profiles and angular outlines, with fresh, un-abraded facets, sockets and edges at sites of block removal. The areal extent of boulder spreads is much larger than that of partially disrupted bedrock: we infer that it is likely that many other macro-scale rock hills have been destroyed by glacial ripping and supplied clasts to boulder spreads.

Jacked and disrupted bedrock

At Forsmark, large excavations previously revealed SHFs, up to 170 m long, filled by 1–80 cm of laminated silt (Carlsson 1979) (Figure 8(A, B)). Sediment fills are common only in the upper 5 m (Carlsson 1979) but are recorded in boreholes to depths of at least 50 m (Follin et al. 2007). Quarries near Iggesund and Kalmar (Figure 8(C–E)) expose similar, gently inclined fractures over 100 m long and with SHF dilation and sediment-fills to depths of 6 m. The presence of open, sediment-filled, SHFs indicates hydraulic jacking of the rock mass under groundwater overpressure (Stephansson and Ericsson 1975). The presence of laminated sediment further suggests deposition by groundwater moving along fracture conduits (Pusch et al. 1990; Leijon 2005). Given the length of some of the sediment-filled fractures at Forsmark, it is likely that sediment infill occurred coeval with jacking. It is
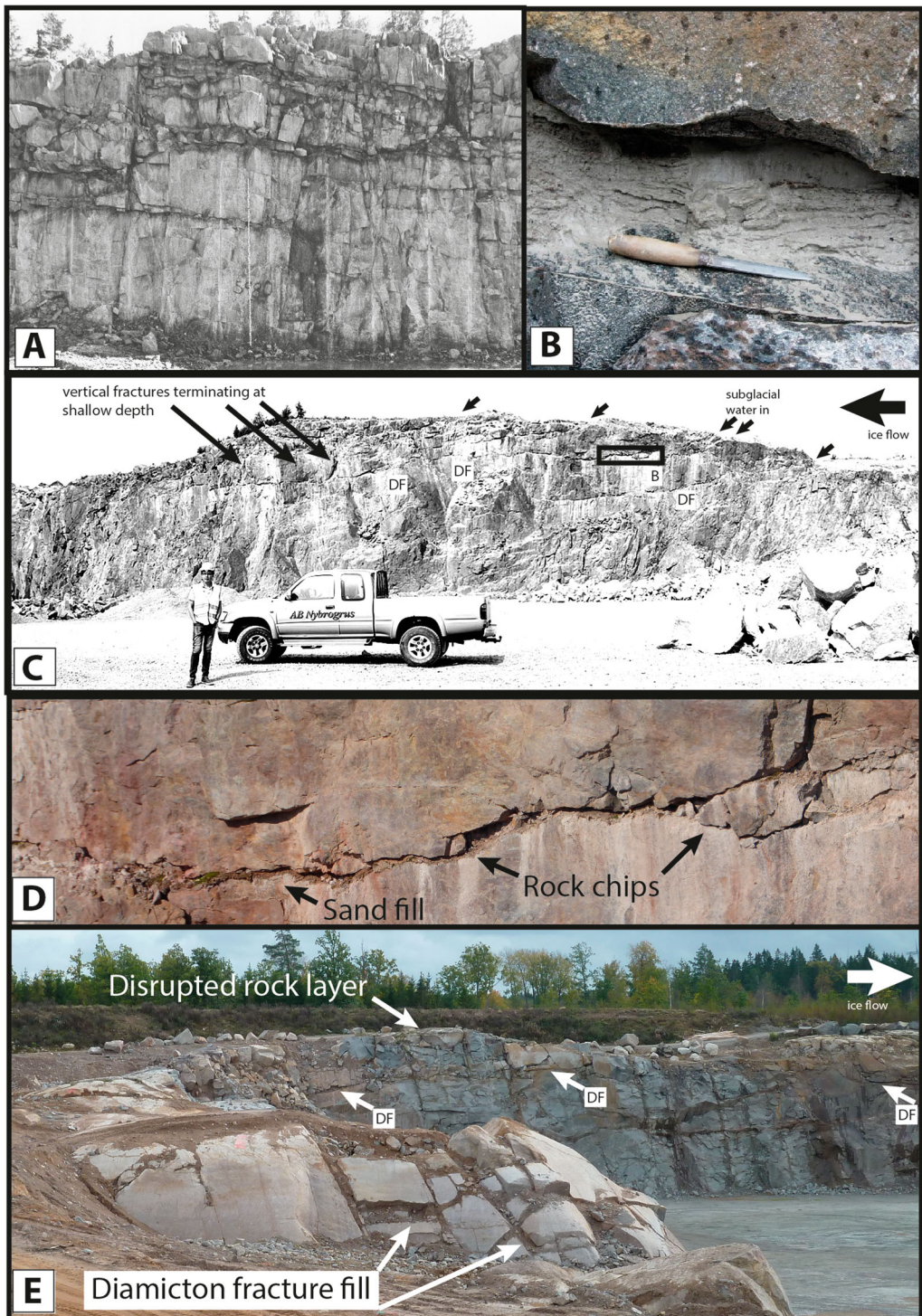
Figure 8. Jacking and disruption. A. Hydraulic jacking and disruption in excavations for the nuclear power station intake canal, Forsmark (Carlsson 1979). The stick is 4 m long. Photo: Göran Hansson. B. Sand and silt fill of dilated sub-horizontal fracture, temporary excavation, Forsmark (Leijon 2005). Photo: Assen Simeonov. C: Hydraulic jacking, fracture dilation and rock disruption in granite gneiss at Runtorp Quarry, Påryd (Figures 1 and 4(G)). West face of the quarry, with dilation and fill of gently-inclined dilated fractures (DF). Box indicates location of image 8D. D. Detail of dilated hydro-fracture showing sand fill <5 cm-thick. E. East face of Runtorp quarry. In the foreground, a small, disrupted roche moutonnée with dilated fractures filled by diamicton. The main face in the background shows inclined, sediment-filled and dilated fractures at the base of a 2–5 m thick disrupted rock layer. Quarry access courtesy of Nybogrus A.B.

not feasible that long (>10–50 m), open fractures as at Forsmark can survive without sediment fill under any effective pressure of the overlying ice sheet.

In plan- and section-views, rock surfaces are seen to be pulled apart, with open, occasionally sediment-filled vertical fractures. Quarry sections, with boulder spreads nearby, show that dilation also affects inclined and sub-vertical fractures so that jacking along SHFs is part of the wider disruption and opening of the near surface bedrock mass (Figure 8(A, E)). In section, open SHFs contain angular rock fragments derived from failure of fracture walls. Alternatively, fills of silt, sand and diamicton may be present (Figure 8(A, D)) (Forssberg et al. 2007). Rock disruption has also been observed beneath thin till covers in excavations (Leijon 2005) and quarries (Figure 8(C)), but whether or not disruption and ripping (and associated block spreads) occur beneath thick till in rock depressions, trenches and valleys remain unknown.

Discussion

Conceptual model for the process sequence of glacial ripping

We propose the following conceptual model for the process sequence that accounts for the boulder spreads in low-relief settings in eastern Sweden (Figure 9).

Stage 1: hydraulic jacking and dilation

Sediment fills in SHFs indicate that hydrostatic pressures at the ice sheet bed were locally sufficiently high to lift rock overburden and overriding ice, to jack open pre-existing fractures (Carlsson 1979; Pusch et al. 1990), and perhaps to propagate SHFs by hydraulic fracturing (Lönnqvist and Hökmark 2013). Where fractures with different orientations were dilated under overpressure the entire near-
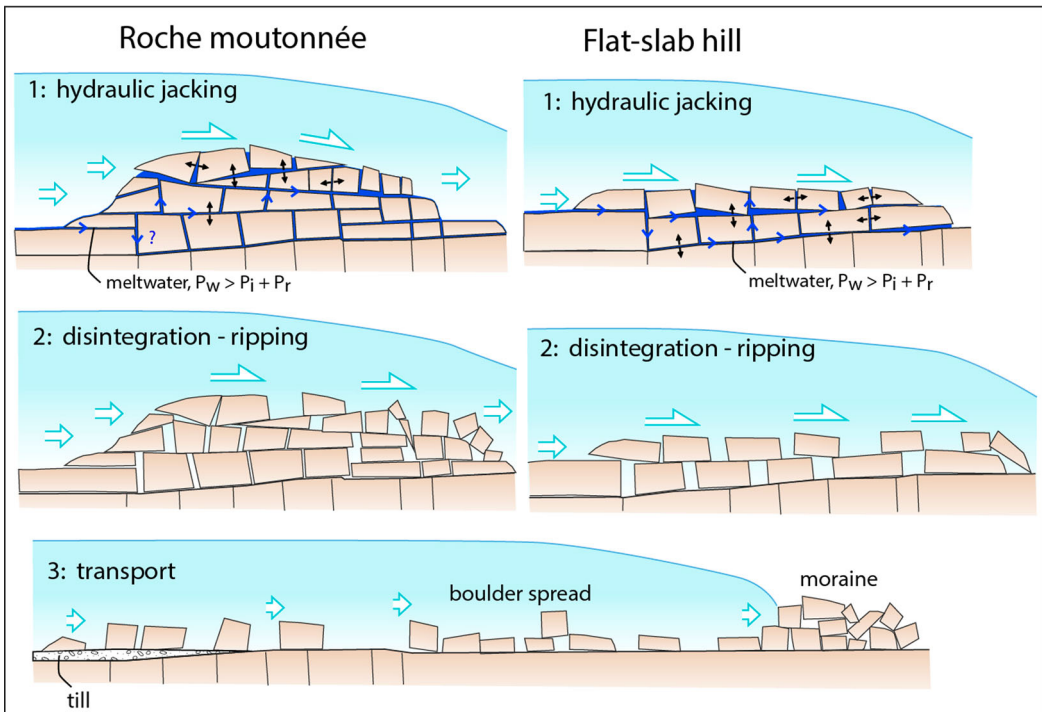
Figure 9. Conceptual model of the sequence of jacking, ripping, transport, and deposition for roches moutonnées (left) and rock sheets (right). Dark blue lines = meltwater. White arrows = ice movement. P_w = water pressure, $P_i + P_r$ is overburden pressure (ice + rock).

surface rock mass was opened. Rock mass dilation was likely rapid and pervasive as punctuated fracture opening leads to dissipation of overpressure.

Stage 2: disruption and disintegration – the ripping process

Where groundwater overpressure resulted in jacking and dilation of fractures, with disruption of the structural fabric of the rock, the static friction along these fractures was reduced and the overall mechanical integrity of the near-surface rock mass was lowered. This friction reduction may have been transient, related to fluctuating water pressures, or permanent, as dilated fractures are locally filled with sediment. When ice traction overcame friction along basal fractures then the rock mass strength of near-surface rock was exceeded, resulting in disintegration and ripping.

Stage 3: transport and deposition

Traction by continuing ice sliding and deformation transported the fragmented blocks, creating boulder spreads emplaced on existing bedrock surfaces or till mantles, with transport distances of a few metres to perhaps a few kilometres. Locally these boulder spreads were pushed to form moraines during minor advances of the ice front.

We envisage the jacking and disruption as necessary precursors to disintegration and actual ripping. Thus, the jacked fractures, the disrupted bedrock (Figure 8) and the disintegrated roches moutonnées and their associated fracture caves (Figure 7) as preserved today should be regarded as aborted stages towards final ripping, where the process sequence of glacial ripping did not reach completion.

The process sequence of glacial ripping likely operated close to the retreating FIS margin because: (1) boulder transport distances were often very short, (2) a lack of boulder edge abrasion (rounding) and the fragility of internally fractured blocks (see also Lundqvist 1987) indicates very limited subglacial transport, and (3) boulder spreads were locally piled into moraine ridges that mark oscillations or standstills of the retreating margin. Sustained and transitory overpressure events have been recorded at the base of the Greenland Ice Sheet in its ablation zone; <50 km from the ice margin (Andrews et al. 2014; Claesson et al. 2016; Wright et al. 2016; Harper et al. 2018). This is consistent with our inference that the process sequence in Sweden occurred close to the rapidly retreating margin of the FIS.

It is possible that both high pressure and high volumes of meltwater are required for hydraulic jacking to occur. The sudden drainage of supraglacial lakes to the ice sheet bed, as has been observed in the Greenland Ice Sheet ablation zone (Das et al. 2008; Doyle et al. 2013), is one potential mechanism for this. The measured uplift of the ice surface immediately after such events demonstrates overpressure conditions at the base. However, multiple overpressure events at the base of the Greenland Ice Sheet have also been measured without supraglacial lake drainage events (Andrews et al. 2014; Wright et al. 2016; Harper et al. 2018). We note that boulder spreads lack any systematic association with eskers or meltwater channels and so do not directly relate to channelled meltwater flow.

Plucking is another process-sequence that involves distinct steps of loosening, entrainment and transport of rock fragments (Rothlisberger and Iken 1981; Iverson 1991). However, glacial ripping is distinct from plucking in its extent, the volumes of rock involved and its integral processes. Plucking is confined to rock steps and releases relatively small numbers of blocks in each plucking event (Figure 3(A)); the deposits/erratics produced by plucking are typically widely spaced, and distinct from the dense boulder spreads described here (Figure 3(B, C)). Glacial ripping affects the near-surface rock mass across wide areas (hundreds of square metres), locally disintegrating and partially or wholly destroying roches moutonnées and similar bedrock hills. Yet the removal of blocks from lee-side faces is a component of ripping, as indicated by angular lee-side faces on roches moutonnées and lee-side boulder trains that occur within boulder spreads. Ripping and plucking may be enhanced under similar conditions of fluctuating groundwater pressure and low overburden pressure beneath thinning ice at retreating margins (Iverson and Person 2012; Sugden et al. 2019).

The first stages of jacking and disruption involve the dilation and disintegration of hard, fractured crystalline rocks. Is the process inherently restricted to such hard rocks? Development of overpressure in sedimentary rocks and sediments is recognized widely from the presence of dilated, sediment-filled fractures (Phillips et al. 2013; Evans et al. 2018). Blow-outs of overpressured subglacial groundwater through sedimentary rocks have been recorded in Alberta and Saskatchewan in Canada, although here a bitumen aquiclude may have played an important role in building up overpressure (Broughton 2018). The Dummer 'moraine' in Ontario contains large slabs (>1 m thick; >10 m long) of layered Ordovician limestone, set within a coarse rubble till of very local origin, and apparently functioning as the 'till factory' of the down-ice Peterborough drumlin field (Shulmeister 1989; Eyles and Doughty 2016). Different models for the Dummer moraine exist, but some form of ripping or 'frontal plucking' is likely (Eyles and Doughty 2016), although the role of subglacial groundwater pressure remains unclear. Comparable 'rip-block' tills, including many boulders of very locally derived Devonian sandstone, are described from northern Scotland (Hall and Whittington 1989). Further investigations are required to model the glaciological scenarios that may lead to jacking, disruption and ripping in different rock types.

As a caveat, whereas we herein identify jacking by water overpressure as a crucial first step towards ripping beneath the warmed-based parts of the FIS in eastern Sweden, it is possible that in other settings different preliminary conditions and processes may also lead to glacial ripping. Some of the features we describe herein are similar to those attributed to cold-ice erosion in Antarctica (Lloyd-Davies et al. 2009), but these were developed at the margin of a land-terminating, cold-based glacier, instead of a marine-lake terminating warm-based ice sheet. Features like ribbed moraines may involve a component of ripping controlled by specific thermal conditions (e.g. Hättestrand and Kleman 1999), with or without fluctuations in water pressure. More widely, freeze-on, or partial thawing of a previously frozen substrate, is commonly invoked to explain various forms of glaciotectonics (e.g. Hambrey and Huddart 1995; Waller and Tuckwell 2005). Many glaciotectonic features are described from ice-marginal zones (Benn and Evans 2010), and have not progressed beyond local disturbance, displacement and transport.

Effectiveness of glacial ripping

Within ripped terrain, rock outcrops are widely spaced, and include partially disrupted roches moutonnées, within extensive boulder spreads. Adjacent glacially roughened and weakly streamlined terrains show limited evidence of ripping. Instead, rock outcrops are dominated by low roches moutonnées that carry smooth, abraded upper surfaces, and show plucked flank- and lee-side cliffs, with till tails in streamlined terrain. Pre-existing roughened and streamlined terrain was modified by ripping that operated late in the last deglaciation, with mobilization of rock and till.

Cosmogenic nuclide inventories are reported for 32 samples from rock surfaces near Forsmark, many from the tops of low roches moutonnées (Hall et al. 2019). In all cases, apparent exposure ages exceed the expected deglaciation ages after correction for postglacial shielding by water. All these rock surfaces retain inherited cosmogenic nuclides from the period before the Late Weichselian glaciation. The interquartile range of simulated total erosion depths over the last 35 ka, including the last ice cover period, is 0.6–1.6 m (Hall et al. 2019). In contrast, depths of erosion on ripped terrain for which we currently lack cosmogenic nuclide data are represented by the 1-4 m depth of boulder spreads. Hence glacial ripping has been capable of eroding depths of rock late in the last glaciation that can exceed estimated depths of rock removed throughout the last glaciation from intact roches moutonnées. Where glacial ripping has operated, cumulative glacial erosion over a glaciation is the sum of (1) continuous abrasion under warm-based, sliding ice, (2) more punctuated plucking and (3) a short-lived phase of ripping at a late stage during deglaciation. In parts of lowland Sweden, glacial erosion by ripping during ice retreat may dominate the erosion budget of an entire glaciation.

The extensive loose rubble presently found in boulder spreads is available for transport in the next glacial cycle. Near-surface rock sheets and roches moutonnées affected by jacking and disruption are

left with greatly reduced rock mass strength. Disrupted and ripped glacial terrains have thus been prepared for deep erosion in the next glacial phase.

Implications and next steps

Several implications emerge from the recognition of glacial ripping as a process sequence driven by groundwater overpressure combined with traction at the ice sheet sole.

(1) Glacial ripping is identified as a highly effective erosion process sequence in hard, fractured bedrock in Sweden. Glacial ripping is likely to occur as a late-stage pulse of erosion, working on surfaces that have been subjected to abrasion and plucking prior to ripping. Bedrock surfaces shaped by abrasion and plucking on low-relief shields in Fennoscandia (Stroeven et al. 2016; Hall et al. 2019; Heyman et al. 2019) and North America (Briner and Swanson 1998) typically yield apparent exposure ages older than regional deglaciation ages, indicating total glacial erosion depths of <3 m over the last 100 ka glacial cycle. In parts of Sweden, in contrast, glacial ripping has mobilized and removed 1-4 m of rock late in the last glaciation and prepared 10 m-high rock hills for removal in the next glaciation. It further appears that glacial ripping represents a late pulse of glacial erosion, unrelated to integrated sliding speed. This means that total erosion depth over a glaciation may not scale with cumulative sliding distance (Näslund et al. 2003; Egholm et al. 2009; MacGregor et al. 2009); see also discussions by Iverson (2002) and Ugelvig et al. (2016). Hence the potential contribution of ripping to glacial erosion budgets is significant but remains to be closely constrained by targeted sampling for cosmogenic nuclides within boulder spreads and on disrupted roche moutonnées.

(2) The extent of boulder spreads indicates that ripping operated widely as the last FIS retreated (Figure 1). Other landforms that may be related to glacial erosion operating late during deglaciation have been reported from other parts of Fennoscandia. These include boulder spreads associated with ribbed moraines (Lundqvist 1989; Sarala 2005) and oblique scarps in rock and till (Harbor et al. 2006; Seppälä 2016) and in murtoo terrain (Mäkinen et al. 2017; Öhrling et al. 2018; Ojala et al. 2019). Further investigation is required to establish the distribution and characteristics of boulder spreads and their links to disrupted bedrock and to other landforms elsewhere in Sweden and on other glaciated shields in the Northern Hemisphere.

(3) Jacking and disruption require groundwater overpressure. Where jacked and disrupted bedrock is preserved, each represents an aborted stage in the proposed process sequence. Hence whilst the entire sequence may occur within a single, short phase of deglaciation, jacking and disruption may also occur earlier during a glaciation. Moreover, the depths of jacked and disrupted bedrock indicate that overpressure sufficient to affect the rock mass strength is limited mainly to the uppermost 10 m of the rock mass. The uppermost rock mass may thus function as a 'safety valve'; dissipating overpressure before it affects deeper parts of the rock mass (see Hökmark et al. 2010 and Lönnqvist and Hökmark 2013 for a discussion of this phenomenon).

(4) The precise glaciological, topographical and geological controls on the distribution of boulder spreads are, at this early stage of research, uncertain. The distribution of boulder spreads and disrupted bedrock in belts and patches in Uppland potentially provides a potential new window on the distribution of groundwater overpressure beneath the FIS during the last deglaciation. Transient development of overpressure may link to drainage of large supraglacial lakes (Dow et al. 2015). Rapid supraglacial lake drainage events deliver vast volumes of water that can trigger dramatic horizontal and vertical acceleration of the ice over periods of 1 d to 1 week (Nienow et al. 2017). High meltwater drainage events from the edge of the FIS are likely recorded by turbidites in the varve chronology of Sweden (De Geer 1940; Strömberg 1989) and in accellerated downcutting events creating subglacial gorges (Jansen et al. 2014). Low magnitude, but high frequency (daily) overpressure events have recently been observed at the base of the Greenland Ice Sheet by pressure transducers installed in boreholes (e.g. Andrews et al. 2014; Wright et al.

2016). Future modelling of the jacking and ripping process sequence has potential to develop our understanding of the complexities of hydrology beneath the FIS and modern ice sheets.

(5) Disrupted roches moutonnées, fracture caves and boulder spreads have previously been used as evidence for high magnitude palaeo-seismic events, supposedly related to glacio-isostatic uplift (Mörner 1978, 2004; Mörner and Sjöberg 2018). Because we show herein that boulder spreads and disrupted roches moutonnées were formed by a subglacial process, these features cannot be used as evidence for high-magnitude earthquakes.

Conclusions

We infer a newly identified process sequence of glacial erosion, termed glacial ripping, whereby intact bedrock is hydraulically jacked and disrupted, disintegrated, transported, and deposited as spreads of large, angular boulders and mega-clasts. Geomorphological evidence for its operation includes 1–4 m thick boulder spreads of large, angular boulders that can extend over areas of >50 km^2, but with glacial transport distances that are commonly restricted to 1–100 m. Boulder spreads occur in terrain where rock masses show extensive fracture dilation in the near surface and disruption and partial disintegration of low rock hills.

Sand and silt fills in fractures indicate jacking and dilation of rock fractures under conditions of groundwater overpressure below the former ice sheet bed. Our hypothesis of boulder spread formation is that, due to jacking, the ice traction overcomes reduced frictional resistance along basal fractures and the rock mass strength of rock sheets and hills is exceeded, resulting in disintegration into blocks and transport of boulders. Short boulder transport distances (<1 km) indicate that the processes involved in ripping developed in the latest stages of the last glaciation close to the retreating ice sheet margin. Plucking is distinct from ripping because it is restricted in its extent, operates mainly at rock cliffs and likely has a different mechanism and, hence, glaciological controls.

Boulder spreads incorporate large volumes of eroded rock. Comparisons with glacial erosion depths derived from cosmogenic nuclide inventories for undisrupted rock surfaces around Forsmark indicate that the 0.6–1.6 m depths of rock removed by abrasion and plucking throughout the last glaciation are less than the 1–4 m of rock lost to ripping late in glaciation.

Glacially disrupted and ripped bedrock is also made ready for removal by future ice sheets. Hence the inferred process sequence of glacial ripping appears to be a highly effective process of glacial erosion.

Having identified glacial ripping and provided a conceptual model for the process sequence, the next steps are to explore further the glaciological and hydrological conditions under which glacial ripping may have occurred. We infer that ripping operated close to the FIS margin during final deglaciation when rapid retreat and very high meltwater fluxes were induced by rapid warming. Even more rapid warming today is driving melting of the Greenland and Antarctic ice sheets and generating subglacial overpressure. Hence glacial ripping may also occur beneath these retreating ice sheet margins.

Acknowledgements

Disclosure statement

Funding

References

Alley R, Cuffey K, Zoet L. 2019. Glacial erosion: status and outlook. Ann Glaciol. 60:1–13.

Andrén T, Lindeberg G, Andrén E. 2002. Evidence of the final drainage of the Baltic Ice Lake and the brackish phase of the Yoldia Sea in glacial varves from the Baltic Sea. Boreas. 31:226–238.

Andrews LC, Catania GA, Hoffman MJ, Gulley JD, Lüthi MP, Ryser C, Hawley RL, Neumann TA. 2014. Direct observations of evolving subglacial drainage beneath the Greenland Ice sheet. Nature. 514:80.

Asch K. 2005. IGME 5000: 1:5 Million International Geological Map of Europe and Adjacent Areas. BGR, Hannover.

Benn DI, Evans DJA. 2010. Glaciers and glaciation. London: Hodder Education. (802 p).

Bergman T, Hedenström A. 2006. Petrographic analysis of gravel and boulders in the Forsmark candidate area. SKB P-06-87. Svensk Kärnbränslehantering AB.

Boulton GS. 1987. Progress in glacial geology during the last fifty years. J Glaciol. 33:25–32.

Briner JP, Swanson TW. 1998. Using inherited cosmogenic ^{36}Cl to constrain glacial erosion rates of the Cordilleran ice sheet. Geology. 26:3–6.

Broughton PL. 2018. Subglacial blowouts in western Canada: insights into extreme meltwater pressures and hydrofracturing. Boreas. 47:326–346.

Carlsson A. 1979. Characteristic features of a superficial rock mass in southern central Sweden – horizontal and sub-horizontal fractures and filling material. Striae. 11:1–79.

Carlsson A, Christiansson R. 2007. Construction experiences from underground works at Forsmark. SKB R-07-10. Svensk Kärnbränslehantering AB.

Carlsten S, Stråhle A. 2000. Borehole radar and BIPS investigations in boreholes at the Boda area. SKB TR-01-02. Svensk Kärnbränslehantering AB.

Chamberlin TC. 1889. The rock-scorings of the great ice invasions. Washington, DC: Government Print Office.

Claesson LL, Kontula A, Harper J, Näslund JO, Selroos JO, Pitkänen P, Puigdomenech I, Hobbs M, Follin S, Hirschorn S. 2016. The Greenland Analogue Project: Final report. SKB TR-14-13. Svensk Kärnbränslehantering AB.

Cunningham FF. 1990. James David forbes, pioneer Scottish glaciologist. Edinburgh: Scottish Academic Press.

Das SB, Joughin I, Behn MD, Howat IM, King MA, Lizarralde D, Bhatia MP. 2008. Fracture propagation to the base of the Greenland Ice sheet during supraglacial Lake drainage. Science. 320:778–781.

De Geer G. 1940. Geochronologia suecica principles. Kungl. sv. vetenskapsakademiens handlingar. 3:367.

Dow CF, Kulessa B, Rutt I, Tsai V, Pimentel S, Doyle S, Van As D, Lindbäck K, Pettersson R, Jones G. 2015. Modeling of subglacial hydrological development following rapid supraglacial lake drainage. J Geophys Res Earth Surf. 120:1127–1147.

Doyle SH, Hubbard A, Dow CF, Jones GA, Fitzpatrick A, Gusmeroli A, Kulessa B, Lindback K, Pettersson R, Box JE. 2013. Ice tectonic deformation during the rapid in situ drainage of a supraglacial lake on the Greenland Ice sheet. Cryosphere. 7:129–140.

Egholm D, Nielsen S, Pedersen VK, Lesemann JE. 2009. Glacial effects limiting mountain height. Nature. 460:884–887.

Evans DJ, Dinnage M, Roberts DH. 2018. Glacial geomorphology of Teesdale, northern Pennines, England: implications for upland styles of ice stream operation and deglaciation in the British-Irish Ice sheet. Proc Geol Assoc. 129:697–735.

Eyles N, Doughty M. 2016. Glacially-streamlined hard and soft beds of the paleo-Ontario ice stream in southern Ontario and New York state. Sediment Geol. 338:51–71.

Follin S, Levén J, Hartley L, Jackson P, Joyce S, Roberts D, Swift B. 2007. Hydrogeological characterisation and modelling of deformation zones and fracture domains, Forsmark modelling stage 2.2. SKB R-07-48. Svensk Kärnbränslehantering AB.

Forssberg O, Hansen LM, Koyi S, Vestgård J, Öhman J, Petersson J, Albrecht J, Hedenström A, Gustavsson J. 2007. Quaternary investigations and GPR measurements at excavated outcrop AFM001264. P-05-269. Svensk Kärnbränslehantering AB.

Glasser NF, Warren CR. 1990. Medium scale landforms of glacial erosion in south Greenland; process and form. Geogr Annal. Series A Phys Geogr. 72:211–215.

Goodfellow BW, Fredin O, Derron MH, Stroeven AP. 2009. Weathering processes and quaternary origin of an alpine blockfield in Arctic Sweden. Boreas. 38:379–398.

Greenwood SL, Clason CC, Nyberg J, Jakobsson M, Holmlund P. 2017. The Bothnian Sea ice stream: early Holocene retreat dynamics of the south-central Fennoscandian Ice sheet. Boreas. 46:346–362.

Hall AM, Ebert K, Goodfellow BW, Hättestrand C, Heyman J, Krabbendam M, Moon S, Stroeven AP. 2019. Past and future impact of glacial erosion in Forsmark and Uppland. SKB TR-19-07. Svensk Kärnbränslehantering AB.

Hall AM, Whittington G. 1989. Late Devensian glaciation of southern Caithness. Scottish J Geol. 25:307–324.

Hambrey MJ, Huddart D. 1995. Englacial and proglacial glaciotectonic processes at the snout of a thermally complex glacier in Svalbard. J Quat Sci. 10:313–326.

Harbor JM, Stroeven AP, Fabel D, Clarhäll A, Kleman J, Li YK, Elmore D, Fink D. 2006. Cosmogenic nuclide evidence for minimal erosion across two subglacial sliding boundaries of the late glacial Fennoscandian ice sheet. Geomorphology. 75:90–99.

Harper J, Humphrey N, Meierbachtol T. 2018. Greenland 'ICE' project, Final Report. SKB R-18-06. Svensk Kärnbränslehantering AB.

Hättestrand, C. & Kleman, J. 1999: Ribbed moraine formation. Quaternary Sci. Rev. 18:43–61.

Heyman J, Goodfellow BW, Stroeven AP, Hall AM, Caffee M, Hättestrand C, Ebert K, Näslund JO, Hippe K, Martel SJ, et al. 2019. Erosion of low-relief basement by the Fennoscandian ice sheet based on bedrock [10]Be and [26]Al. Conference Abstract, INQUA, Dublin.

Hökmark H, Lönnqvist M, Fälth B. 2010. THM-issues in repository rock. Thermal, mechanical, thermo-mechanical and hydro-mechanical evolution of the rock at the Forsmark and Laxemar sites. SKB TR-10-23. Svensk Kärnbränslehantering AB.

Iverson NR. 1991. Potential effects of subglacial water-pressure fluctuations on quarrying. J Glaciol. 37:27–36.

Iverson NR. 2002. Processes of glacial erosion. In: Menzies J., editor. Modern and past glacial environments. Amsterdam: Elsevier; p. 131–145.

Iverson NR, Person M. 2012. Glacier-bed geomorphic processes and hydrologic conditions relevant to nuclear waste disposal. Geofluids. 12:38–57.

Jansen JD, Codilean AT, Stroeven AP, Fabel D, Hättestrand C, Kleman J, Harbor JM, Heyman J, Kubik PW, Xu S. 2014. Inner gorges cut by subglacial meltwater during Fennoscandian ice sheet decay. Nat Commun. 5:3815.

Kleman J. 1990. On the use of glacial striae for reconstruction of paleo-ice sheet flow patterns. Geogr Annal. 72A:217–236.

Kleman J, Borgström I. 1990. The boulder fields of Mt. Fulufjället, west-central Sweden: late Weichselian boulder blankets and interstadial periglacial phenomena. Geogr Annal Series A Phys Geogr. 72:63–78.

Kleman J, Stroeven AP, Lundqvist J. 2008. Patterns of Quaternary ice sheet erosion and deposition in Fennoscandia and a theoretical framework for explanation. Geomorphology. 97:73–90.

Krabbendam M, Bradwell T. 2014. Quaternary evolution of glaciated gneiss terrains: pre-glacial weathering vs. glacial erosion. Quat Sci Rev. 95:20–42.

Krabbendam M, Glasser NF. 2011. Glacial erosion and bedrock properties in NW Scotland: abrasion and plucking, hardness and joint spacing. Geomorphology. 130:374–383.

Lagerbäck R, Sundh M, Svedlund J-O, Johansson H. 2005. Forsmark site investigation Searching for evidence of late-or post-glacial faulting in the Forsmark region. SKB R-05-51. Svensk Kärnbränslehantering AB.

Leijon B. 2005. Forsmark site investigation: Investigations of superficial fracturing and block displacements at drill site 5. SKB P-05-199. Svensk Kärnbränslehantering AB.

Lloyd-Davies MT, Atkins CB, Van der Meer JJM, Barrett PJ, Hicock SR. 2009. Evidence for cold-based glacial activity in the Allan Hills, Antarctica. Quat Sci Rev. 28:3124–3137.

Lönnqvist M, Hökmark H. 2013. Approach to estimating the maximum depth for glacially induced hydraulic jacking in fractured crystalline rock at Forsmark, Sweden. J Geophys Res Earth Surf. 118:1777–1791.

Lundqvist G. 1940. Bergslagens minerogena jordarter. Sveriges Geologiska Undersökning Serie C Avhandlingar Och Uppsatser. 433:1–87.

Lundqvist J. 1986. Late Weichselian glaciation and deglaciation in Scandinavia. Quat Sci Rev. 5:269–292.

Lundqvist J. 1987. Glaciodynamics of the younger dryas marginal zone in Scandinavia: implications of a revised glaciation model. Geogr Annal Series A Phys Geogr. 69:305–319.

Lundqvist J. 1989. Rogen (ribbed) moraine—identification and possible origin. Sediment Geol. 62:281–292.

Lundqvist J. 2007. Surging ice and break-down of an ice dome - a deglaciation model for the Gulf of Bothnia. GFF. 129:329–336.

MacGregor KR, Anderson RS, Waddington ED. 2009. Numerical modeling of glacial erosion and headwall processes in alpine valleys. Geomorphology. 103:189–204.

Mäkinen J, Kajuutti K, Palmu J-P, Ojala A, Ahokangas E. 2017. Triangular-shaped landforms reveal subglacial drainage routes in SW Finland. Quat Sci Rev. 164:37–53.

Mörner N-A. 1978. Faulting, fracturing, and seismicity as functions of glacio-isostasy in Fennoscandia. Geology. 6:41–45.

Mörner N-A. 2004. Active faults and paleoseismicity in Fennoscandia, especially Sweden. Primary structures and secondary effects. Tectonophysics. 380:139–157.

Mörner N-A, Einar Tröften P, Sjöberg R, Grant D, Dawson S, Bronge C, Kvamsdal O, Sidén A. 2000. Deglacial paleoseismicity in Sweden: the 9663 BP Iggesund event. Quat Sci Rev. 19:1461–1468.

Mörner N-A, Sjöberg R. 2018. Merging the concepts of pseudokarst and paleoseismicity in Sweden: A unified theory on the formation of fractures, fracture caves, and angular block heaps. Int J Speleol. 47:10.

Näslund JO, Rodhe L, Fastook JL, Holmlund P. 2003. New ways of studying ice sheet flow directions and glacial erosion by computer modelling–examples from Fennoscandia. Quat Sci Rev. 22:245–258.

Nienow P, Sole A, Slater D, Cowton T. 2017. Recent advances in our understanding of the role of meltwater in the Greenland ice sheet system. Curr Clim Change Rep. 3:330–344.

Öhrling C, Peterson G, Mikko H. 2018. Detailed geomorphological analysis of LiDAR derived elevation data, Forsmark. SKB R-18-10. Svensk Kärnbränslehantering AB.

Ojala AE, Peterson G, Mäkinen J, Johnson MD, Kajuutti K, Palmu J-P, Ahokangas E, Öhrling C. 2019. Ice-sheet scale distribution and morphometry of triangular-shaped hummocks (murtoos): a subglacial landform produced during rapid retreat of the Scandinavian Ice sheet. Ann Glaciol. 60:1–12.

Olvmo M, Johansson M. 2002. The significance of rock structure, lithology and pre-glacial deep weathering for the shape of intermediate-scale glacial erosional landforms. Earth Surf Process Landforms. 27:251–268.

Patton H, Hubbard A, Andreassen K, Auriac A, Whitehouse PL, Stroeven AP, Shackleton C, Winsborrow M, Heyman J, Hall AM. 2017. Deglaciation of the Eurasian ice sheet complex. Quat Sci Rev. 169:148–172.

Persson C. 1992. The latest ice recession and till deposits in northern Uppland, eastern central Sweden. SGU Bull. 81:217–224.

Phillips E, Everest J, Reeves H. 2013. Micromorphological evidence for subglacial multiphase sedimentation and deformation during overpressurized fluid flow associated with hydrofracturing. Boreas. 42:395–427.

Pusch R, Börgesson L, Knutsson S. 1990. Origin of silty fracture fillings in crystalline bedrock. Geologiska Föreningen i Stockholm Förhandlingar. 112:209–213.

Rea BR, Whalley WB, Rainey MM, Gordon JE. 1996. Blockfields: old or new? Evidence and implications from some plateau blockfields in northern Norway. Geomorphology. 15:109–121.

Rothlisberger H, Iken A. 1981. Plucking as an effect of water-pressure variations at the glacier bed. Ann Glaciol. 2:57–62.

Sandström B, Tullborg E-L. 2009. Episodic fluid migration in the Fennoscandian shield recorded by stable isotopes, rare earth elements and fluid inclusions in fracture minerals at Forsmark, Sweden. Chem Geol. 266:126–142.

Sarala P. 2005. Glacial morphology and dynamics with till geochemical exploration in the ribbed moraine area of Peräpohjola, Finnish Lapland. Espoo: Geological Survey of Finland. 17 p.

Seppälä MVJ. 2016. Lidar-Based detection and interpretation of glaciotectonic features of the morainic topography of Finland. J Geol Res. 2016:1–11.

Shulmeister J. 1989. A conceptual model for the deposition of the Dummer moraine, southern Ontario. Geomorphology. 2:385–392.

Sjöberg R. 1986. Caves indicating neotectonic activity in Sweden. Geogr Annal. Series A Phys Geogr. 68:393–398.

Stephansson O, Ericsson B. 1975. Pre-Holocene joint fillings at Forsmark, Uppland, Sweden. GFF. 97:91–95.

Stephens MB. 2010. Forsmark site investigation. Bedrock geology – overview and excursion guide. SKB R-10-04. Svensk Kärnbränslehantering AB.

Stroeven AP, Hättestrand C, Kleman J, Heyman J, Fabel D, Fredin O, Goodfellow BW, Harbor JM, Jansen JD, Olsen L, et al. 2016. Deglaciation of Fennoscandia. Quat Sci Rev. 147:91–121.

Strömberg B. 1989. Lat.e Weichselian deglaciation and clay varve chronology in east-central Sweden. Sveriges Geologiska Undersökning. Serie Ca. 73:1–70.

Strömberg B. 1994. Younger Dryas deglaciation at Mt. Billingen, and clay varve dating of the Younger Dryas/preboreal transition. Boreas. 23:177–193.

Sugden DE, Hall AM, Phillips WM, Stewart M. 2019. Plucking enhanced beneath ice sheet margins: evidence from the Grampian Mountains, Scotland. Geogr Annal Series A Phys Geogr. 101:34–44.

Terry JP, Goff J. 2014. Megaclasts: proposed revised nomenclature at the coarse end of the udden-wentworth grain-size scale for sedimentary particles. J Sediment Res. 84:192–197.

Ugelvig SV, Egholm DL, Iverson NR. 2016. Glacial landscape evolution by subglacial quarrying: A multiscale computational approach. J Geophys Res: Earth Surf. 121:2042–2068.

Waller RI, Tuckwell GW. 2005. Glacier-permafrost interactions and glaciotectonic landform generation at the margin of the Leverett Glacier, West Greenland. Geol Soc London. 242:39–50.

Wänstedt S. 2000. Geophysical and geological investigations of the Boda area. SKB R-00-23. Svensk Kärnbränslehantering AB.

Wright PJ, Harper JT, Humphrey NF, Meierbachtol TW. 2016. Measured basal water pressure variability of the western Greenland ice sheet: implications for hydraulic potential. J Geophys Res Earth Surf. 121:1134–1147.